Tailoring butane-1,2,3,4-tetraol-based maltosides (BTMs) via group-swapping and unsymmetry: New detergent design strategies for membrane protein studies

Taeyeol Youn,[a,‡] Muhammad Ehsan,[a,‡] Parameswaran Hariharan,[b] Xianglan Li,[c] Bernadette Byrne,[d] Xiangyu Liu,[c] Lan Guan,[b] and Pil Seok Chae[a,*]

[a] Major in Bionano Engineering, School of Bio-Pharmaceutical Convergence, Hanyang University, Ansan, 155-88, Republic of Korea

[b] Department of Cell Physiology and Molecular Biophysics, Center for Membrane Protein Research, School of Medicine, Texas Tech University Health Sciences Center, Lubbock, Texas 79430, United States

[c] State Key Laboratory of Membrane Biology, Tsinghua-Peking Center for Life Sciences, Beijing Frontier Research Center for Biological Structure, School of Pharmaceutical Sciences, Tsinghua University, Beijing 100084, China

[d] Department of Life Sciences, Imperial College London, London SW7 2AZ, U.K.

[‡]These authors contributed equally.

Abstract

Membrane proteins are essential bio-macromolecules involved in numerous critical biological processes and serve as therapeutic targets for a wide range of modern pharmaceuticals. Small amphipathic molecules, called detergents or surfactants, are widely used for the isolation and structural characterization of these proteins. A key requirement for such studies is the ability to maintain membrane protein stability in aqueous solution, a task where conventional detergents often fall short. While many new detergents have been developed based on novel molecular scaffolds, comparatively little effort has been made to enhance detergent performance through rational modification of existing structures, largely due to the limited availability of guiding design principles and strategies. In this study, we refined previously developed butane-1,2,3,4-tetraol based maltosides (BTMs), using two structural modification strategies, head/tail group-swapping and the introduction of hydrophobic unsymmetry. The resulting group-swapped (GS)-BTMs exhibited distinctive physical properties compared to the original BTM, including differences in water-solubility, critical aggregation concentration, and self-assembly size. When evaluated with model membrane proteins, including the human adrenergic receptor (β_2AR), symmetric GS-BTMs (e.g., GS-BTM-C11 and GS-BTM-C12) showed superior performance relative to the original BTM-C11 and the benchmark detergents (DDM and LMNG). The unsymmetric variants, such as GS-BTM-C14,10 and GS-BTM-C15,9, further improved protein stability. These findings highlight group-swapping and hydrophobic unsymmetry as effective strategies for enhancing detergent performance. This work demonstrates how minimal structural modification can impact detergent properties and efficacy, offering valuable insights for the development of improved detergents from existing molecular frameworks.

Introduction

Membrane proteins play a critical role in a wide range of biological processes.[1] These bio-macromolecules are essential for maintaining cellular function and are implicated in numerous human diseases resulting from protein deficiencies, mutations, or other abnormalities.[2-4] As a result, membrane proteins have become primary targets for the pharmaceutical industry, and a mechanistic understanding of these biomolecules holds great promise for drug discovery and development.[5-7] High resolution, three-dimensional atomic structures of membrane proteins not only deepen our understanding of their molecular mechanisms, but also facilitate structure-based drug design. To carry out structural investigation, membrane-embedded proteins must first be extracted from cellular membranes.[8] Commonly used detergents for this purpose include OG (*n*-octyl-β-D-glucoside), DM (*n*-decyl-β-D-maltoside), and DDM (*n*-dodecyl-β-D-maltoside) and LDAO (lauryldimethylamine-*N*-oxide). These conventional detergents have contributed to the characterization of approximately 70% of all known membrane protein structures.[9] However, traditional detergents that have a single head and tail group often fail to stabilize more challenging membrane proteins, such as those derived from eukaryotic cells or those forming large multi-subunit complexes. Accordingly, many membrane proteins tend to denature/aggregate in aqueous solution when solubilized with these detergents, hindering downstream functional assays, spectroscopic analysis or crystallization efforts.[10] This underscore the urgent need for novel amphiphilic agents capable of better stabilizing membrane proteins for structural studies.

Over the past few decades, significant efforts have been made to develop alternative membrane mimetic systems, such as bicelles,[11] amphipols (e.g., APols),[12] peptide-based detergents (e.g., lipopeptide detergents and *β*-peptides),[13,14] and nanoassemblies stabilized by peptides (e.g., saposin A),[15] membrane scaffold proteins,[16] or polymers (e.g., styrene-maleic acid (SMA)[17] and diisobutylene-maleic acid (DIBMA)[18]). While these systems have been successfully used for cryo-EM based structural studies of membrane proteins, their use in protein extraction and crystallization remains limited. Detergents, by contrast, are widely employed throughout all stages of membrane protein research from extraction, purification to structure determination. In response to the limitations of traditional detergents, a variety of novel amphiphiles have been developed, as exemplified by lauryl maltose neopentyl glycol (LMNG),[19] octyl glucose neopentyl glycols (OGNG),[20] and glyco-diosgenin (GDN),[21] and other carbohydrate-based detergents.[22-26] Some of these novel detergents have significantly advanced membrane protein structure determination; for instance, LMNG and GDN have contributed to the determination of 450 high resolution membrane protein structures during the past decade.[9] These tools have proven especially effective for stabilizing biologically and pharmaceutically relevant membrane proteins, such as G protein-coupled receptors (GPCRs) and ATP-binding cassette (ABC) transporters.[9] Compared to other membrane mimetic systems like nanodiscs (NDs) and bicelles, small amphiphilic agents offer the added advantage of being compatible with all three major techniques for protein structure determination: X-ray crystallography, nuclear magnetic resonance (NMR) spectroscopy and cryogenic electron microscopy (cryo-EM). Additionally, their chemical structures can be readily modified to optimize performance, making them highly adaptable for membrane protein research.

Recently, new detergents have been developed thorough diverse synthetic strategies, including combinatorial synthesis,[27] two-dimensional expansion synthesis,[28] and multi-component synthesis.[29] Theses approaches not only streamline the synthetic process but also expand the chemical diversity of detergents through diversity-oriented design. Nonetheless, rather than merely increasing the number or chemical space of detergents, it is crucial to rationally design molecules specifically suited for membrane protein structural studies. In this context, a recent strategy known as complementary and metric-assisted detergent design has emerged, offering a rational approach to optimizing detergent properties.[30,31] Despite a growing number of detergent development efforts, rational design remains rare and challenging due to our limited understanding of fundamental design principles. In this manuscript, we present a case study of detergent optimization using two design strategies: group-swapping (the exchange of detergent head and tail groups) and detergent unsymmetry (incorporating two distinct alkyl chains). Following these strategies, we designed and synthesized a series of new amphiphiles derived from previously developed detergents, butane-1,2,3,4-tetraol based maltosides (BTMs) (**Figure 1**).[32] These variants, referred to as group-swapped (GS)-BTMs, demonstrated superior stabilization of model membrane proteins, including β_2AR, compared to the gold standard DDM, LMNG, and the parent BTM. Our findings reveal that group-swapping is a promising strategy for enhancing detergent performance in membrane protein stabilization. Furthermore, unsymmetric versions of GS-BTMs, featuring two different alkyl chains, showed even greater stabilization efficacy than their symmetric counterparts. The newly developed GS-BTMs represent valuable tools for advancing membrane protein structural studies and the group-swapping strategy introduced here offers a novel route for rational detergent optimization in this field.

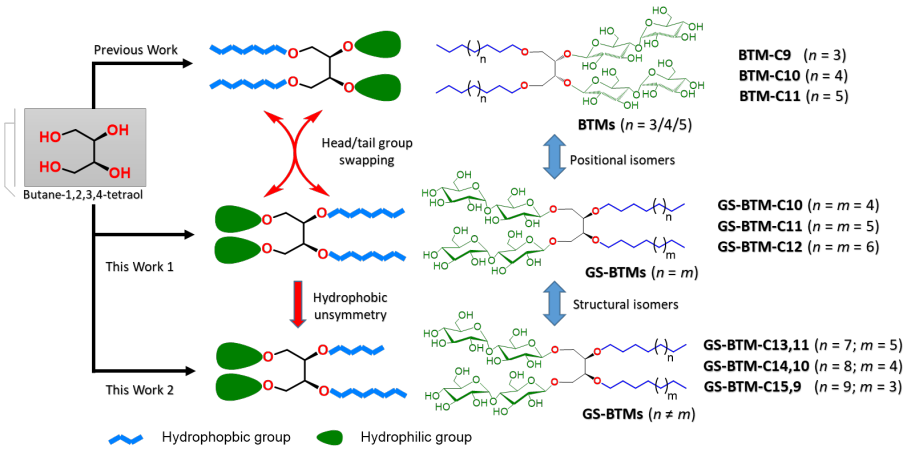


Figure 1. Schematic representations of previously reported butane-1,2,3,4-tetraol derived maltosides with two C11 alkyl chains (BTM-C11) (*top*), and newly prepared GS-BTMs (*middle* and *bottom*). The GS-BTMs are categorized as

either symmetric (n = m; identical alkyl chains) or unsymmetric (n ≠ m; two different alkyl chains). The unsymmetric GS-BTMs were developed by introducing hydrophobic unsymmetry into the symmetric variants, which themselves were derived from the original BTM structure through a group-swapping strategy. The alkyl chain length in the GS-BTMs range from C10 to C12. All unsymmetric GS-BTMs were derived from GS-BTM-C12, and thus possess a total 24 carbon atoms in the lipophilic region (e.g., C13+C11, C14+C10, and C15+C9).

Results and Discussion

Detergent Design, Synthesis and Physical Characterizations

Previously, we developed a series of BTMs featuring two maltoside head groups and two alkyl chains connected via the butane-1,2,3,4-tetraol (BT) linker (**Figure 1**).[32] These amphiphilic BTMs exhibited varying abilities to stabilize membrane proteins, depending on the chirality of the BT linker. Among them, BTM-C11, derived from the meso-isomer of the BT linker, showed the highest efficacy for protein stabilization. The central BT linker contains two distinct types of hydroxyl groups; terminal primary and internal secondary alcohols. This structural feature prompted us to explore the impact of exchanging the positions of the head and tail groups in the BTMs, leading to the design of a new class of detergents, termed the GS-BTMs (Figure 1). In these new constructs, the two alkyl chains are attached to the internal secondary alcohols the BT linker instead of the terminal primary alcohols, as in the original BTMs. We hypothesized that this inversion would reduce the inter-alkyl chain distance, increase packing density in micelle interiors and consequently enhance membrane protein stabilization. In addition, this group swapping is expected to influence the conformational flexibility of the head and tail groups.[33] Based on the nature of the alcohols involved in the attachments, primary for the head groups and secondary for the tail groups in the GS-BTMs, this modified architecture likely increases the flexibility of the hydrophilic head groups, while reducing that of the hydrophobic tail groups, relative to the original BTMs. While the structural change from the BTM to the GS-BTM appears minimal, we hypothesized that it would significantly affect detergent properties and biological performance. This is because detergent self-assemblies, micelles, which form in aqueous solution, rather than individual moleculesinteract directly with membrane proteins. Previous studies highlighted the profound impact that even subtle structural variations in amphiphiles can have on self-assembly morphology and behavior. For example, Stupp et al.[34] demonstrated that peptide amphiphile isomers with identical compositions but different amino acid sequences self-assembled into distinct chiral nanostructures. Perttu, et al. developed inverse phosphocholine (iPC) lipids by swapping the positions of the positively charged quaternary amine and the negatively charged phosphate groups in standard phosphocholine (PC) lipids.[35] This rearrangement led to changes in liposome release kinetics. Similarly, Gimeno-Ferrero et al. reported small alkenyl lipids whose self-assembly structures shifted upon swapping their head and tail groups.[36] In the cases of iPC and alkenyl lipids, the group exchange induced significant structural changes — charge inversion and altered head/tail group numbers, respectively. In contrast, the BTM-to-GS-BTM transformation involved swapping two neutral groups of equal number, resulting in only a subtle structural alteration. Notably, unlike the iPC and alkenyl lipid studies, which focused solely on self-assembly structures, we evaluated both the GS-BTM self-assembly structures and their ability to

solubilize and stabilize multiple model membrane proteins. To further explore the structural design space, we also introduced unsymmetry into the hydrophobic region of the GS-BTMs by incorporating two different alkyl chains, a strategy referred to as 'detergent unsymmetry'. This design was inspired by prior studies on MNGs and TTGs where unsymmetric detergents (e.g., MNG-8,12 and TTG-8,12) outperformed their symmetric counterparts (MNG-10,10 and TTG-10,10) in membrane protein stabilization.[37,38]

In developing the GS-BTMs, we systematically varied the alkyl chain length from C10 to C12, producing GS-BTM-C10, GS-BTM-C11, and GS-BTM-C12. This variation aimed to optimize the hydrophilic-lipophilic balance (HLB), a key parameter for membrane protein stabilization. According to Griffin's method,[39] these GS-BTMs have HLB values ranging from 12.3 to 13.0, slightly lower than those of DDM (13.4) and LMNG (13.6), yet still within the optimal range of 11–14.[30] We also designed three unsymmetric GS-BTMs, GS-BTM-C13,11, GS-BTM-C14,10 and GS-BTM-C15,9, each containing two different alkyl chains but maintaining a total of 24 carbon atoms in the lipophilic region, equivalent to GS-BTM-C12. Consequently, all these unsymmetric detergents share the same HLB value as GS-BTM-C12. We chose not to pursue GS-BTMs with greater unsymmetry (e.g., GS-BTM-C18,6) as excessively long alkyl chains could impair membrane protein stabilization. Altogether, these symmetric and unsymmetric alkyl chain variants provide a useful strategy to fine-tune detergent properties, particularly HLB and hydrophobic length — two critical factors in membrane protein stabilization. Notably, the detergent's hydrophobic length must align with the hydrophobic thickness of membrane protein surfaces (approximately 28–32 Å) to ensure optimal compatibility and support protein stability.

The syntheses of the GS-BTMs were accomplished using a strategy based on the previously reported BTM preparation protocol (**Figure 2a**). Benzyl protected diol derivative (**A**) served as the key scaffold for introduction of alkyl chains, either symmetric or unsymmetric, — using sodium hydride (NaH) in DMF. Subsequent removal of the benzyl protecting groups was achieved via hydrogenation with H_2 over palladium on carbon (Pd/C), yielding the dialkylated diol intermediates (**B**). These intermediates were then subjected to AgOTf-promoted glycosylation for maltoside head group installation, followed by global deprotection using sodium methoxide (NaOMe). The synthetic route is straightforward and efficient, allowing the GS-BTMs to be prepared in multigram quantities. The chemical structures of all GS-BTMs were confirmed by NMR spectroscopy and mass spectrometry. In the ^{1}H NMR spectra, GS-BTM-C11 and GS-BTM-C13,11 exhibited a single doublet peak at 4.33 ppm, in contrast to the two distinct doublets observed for the β-anomeric protons of BTM-C11. This chemical shift, along with the observed vicinal coupling constants ($^3J_{aa}$ = of 8.0 Hz), supports the formation of β-glycosidic linkages (**Figure 2b, S1**†). The transition from the two doublets to a single double in the GS-BTMs is likely due to the decreased spatial separation between the maltose head group and the chirality centers in the BT linker compared to the original BTM. Additionally, decreased conformational flexibility of the maltoside head group in the GS-BTMs amy also contribute to this spectral change. The ^{13}C NMR spectra of the GS-BTMs showed two β-anomeric carbon peaks at 104.2 and 103.0 ppm, consistent with a β-glycosidic configuration (**Figure 2c**). Notably, detergent unsymmetry had little effect on the chemical shifts and splitting patterns of both

anomeric protons and carbons in the ^{1}H and ^{13}C NMR spectra. Furthermore, the terminal methyl proton signals (CH_3) in the ^{1}H NMR spectra of the unsymmetric GS-BTMs, GS-BTM-C13,11, GS-BTM-C14,10 appeared similar to those of the symmetric GS-BTM-C11. However, in the case of GS-BTM-C15,9, which possesses the greatest degree of unsymmetry among the three GS-BTMs, a slight differentiation was observed for the two terminal methyl protons signals (**Fig. S2**†).

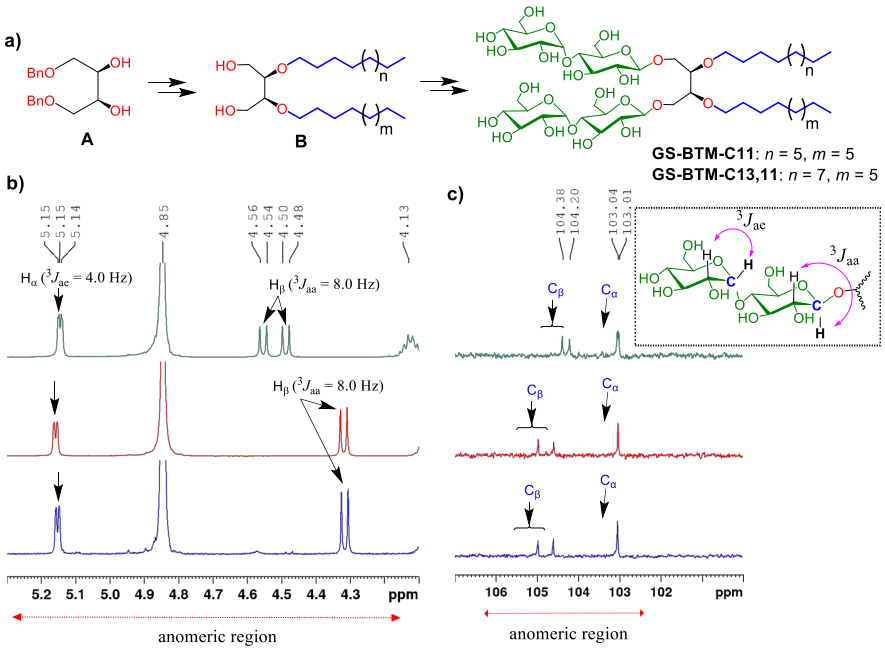


Figure 2. (a) Synthetic scheme for the preparation of representative GS-BTMs (GS-BTM-C11 and GS-BTM-C13,11). Both GS-BTMs were synthesized from benzyl protected *cis*-diol compound (compound **A**) which was subjected to alkylation and subsequent benzyl deprotection to yield the diol-functionalized compound **B**. The maltoside head group was then attached via glycosylation at the primary alcohol position of compound **B** , followed by global deprotection. (b,c) ^{1}H and ^{13}C NMR spectra of BTM-C11 (*top*), GS-BTM-C11 (*middle*), and GS-BTM-C13,11 (*bottom*), focusing on the anomeric region (4.2–5.3 ppm for ^{1}H NMR and 100–106 ppm for ^{13}C NMR). Full spectra are provided in Fig. S1†. BTM-C11 displayed two doublets at ~ 4.5 ppm, corresponding to the β-anomeric protons, while GS-BTM-C11 and GS-BTM-C13,11 exhibited a single doublet at ~ 4.3 ppm. Vicinal coupling constants of β and α-anomeric protons ($^{3}J_{aa}$ and $^{3}J_{ae}$, respectively) are indicated above each peak. The β and α-anomeric carbon signals appeared at ~104.5 and ~102.5 ppm, respectively. C_α/C_β and H_α/H_β denote the anomeric carbons and protons), respectively, as indicated in the chemical structure of the maltoside head group (*right*).

The newly synthesized GS-BTMs exhibited improved water-solubility compared to their BTM counterparts. All GS-BTMs were highly water-soluble (>10%), with the exception of GS-BTM-12, which displayed a lower water solubility of ~7 wt%. This enhanced water-solubility is likely attributable to the increased conformational flexibility of the maltoside head group in the GS-BTMs relative to the BTMs. Additional increases in water-solubility were observed by the introduction of detergent unsymmetry. These results indicate that both head/tail group swapping and hydrophobic unsymmetry contribute positively to detergent water-solubility within this molecular scaffold. All detergent solutions remained stable at room temperature for over a month, a critical requirement for biological applications. We investigated the properties of the GS-BTMm self-assemblies by measuring critical aggregate concentrations (CACs) and hydrodynamic radii (R_h). CACs were determined via encapsulation of the water-insoluble dye (diphenylhexatriene (DPH))[40] in micelle interiors, while R_h values were obtained by dynamic light scattering (DLS). These data are summarized in **Table 1**. As expected from their dual alkyl chain structures, the CACs of the GS-BTMs were significantly lower than that of the single alkyl-chained DDM (0.17 mM). Except for GS-BTM-C10, all GS-BTMs exhibited CAC values lower than that of LMNG (10 μM), indicating a higher propensity to self-assemble in aqueous solution. Among the symmetric GS-BTMs, CACs decreased with increasing alkyl chain length, from 15 μM (C10) to 7 μM (C12). For the unsymmetric version, CACs tended to decrease as difference in alkyl chain length increased, with the lowest CAC (7 μM) observed for GS-BTM-C15,9. This trend mirrors observations from previous studies on unsymmetric MNG detergents and supports the notation that detergent unsymmetry enhances the tendency to self-assemble. Similarly, self-assembly sizes varied depending on alkyl chain length and detergent unsymmetry. For the symmetric GS-BTMs (GS-BTM-C10, C11, and C12), aggregate sizes increased with alkyl chain length. Specifically, GS-BTM-C10 formed the smallest assemblies, comparable in size to those of DDM, while GS-BTM-C12 formed the largest, exceeding even those of LMNG. Introduction of unsymmetry into the hydrophobic region led to dramatic decreases in self-assembly sizes. R_h values dropped from 17.1 nm (GS-BTM-C12) to 13.0 nm (GS-BTM-C13,11) and further to 4.4 nm and 4.1 nm for GS-BTM-C14,10 and GS-BTM-C15,9, respectively. This trend is consistent with previous findings on unsymmetric MNGs and underscores the effectiveness of hydrophobic unsymmetry in reducing detergent assembly size. The observed size reduction is attributable to changes in the critical packing parameter (CPP), which reflects the relative volumes of the detergent head and tail groups.[41] Detergent unsymmetry reduces CPP and thereby favors the formation of smaller self-assemblies a feature advantageous for membrane protein structural studies. To assess assembly homogeneity, we analyzed the size distributions of GS-BTM aggregates via DLS. Number- or volume-weighted DLS profiles displayed a single, uniform size distribution for all GS-BTMs, while intensity-weighted DLS profiles revealed the presence of small fractions of larger aggregates in most GTMs (**Figures S3a & S4a**†). Interestingly, the two unsymmetric GS-BTMs (GS-BTM-C14,10 and GS-BTM-C15,9) exhibited only small assemblies even in the intensity-weighted DLS profile, indicating their enhanced micelle homogeneity (**Figure 3a,b**).

Table 1. Molecular weights (MWs), critical micelle concentrations (CACs), hydrodynamic radii (R_h; n = 5) and water-solubility of the GS-BTMs, along with three controls (BTM-C11, LMNG and the conventional detergent DDM).

Detergent	*M.W.*[a]	CMC (mM)	CMC (wt%)	R_h (nm)[b]	Water-solubility (wt%)
GS-BTM-C10	1051.22	~0.015	~0.0016	3.8±0.1	>10
GS-BTM-C11	1079.28	~0.009	~0.0010	4.9±0.2	>10
GS-BTM-C12	1107.33	~0.007	~0.0008	17.1±0.4	~7
GS-BTM-C13,11	1107.33	~0.006	~0.0007	13.0±1.2	~10
GS-BTM-C14,10	1107.33	~0.006	~0.0007	4.4±0.1	>10
GS-BTM-C15,9	1107.33	~0.005	~0.0006	4.1±0.1	>10
BTM-C11	1079.3	~0.008	~0.009	4.7±0.3	~10
LMNG	1005.20	~0.010	~0.001	9.8 ±0.2	~10
DDM	510.6	~0.17	~0.0087	3.4±0.1	~10

[a]Molecular weight of detergents. [b]Hydrodynamic radii of micelles were determined at 1.0 wt% by dynamic light scattering

The concentration-dependent behavior of aggregates formed by the symmetric and unsymmetric GS-BTMs was further investigated by varying detergent concentration. As previously reported, DDM aggregates maintained a constant size across the concentration range of 0.1 wt% to 1.0 wt%, while BTM-C11 and LMNG exhibited slight and substantial increases in aggregate size, respectively, under the same variation (**Fig. 3c**). This concentration-dependent variation appears to correlate with inherent size of detergent aggregates. For example, GS-BTM-C10, which forms small micelles, showed negligible changes in aggregate size, a similar trend to DDM. In contrast, GS-BTM-C12, which forms larger aggregates showed a pronounced increase in size increasing detergent concentration, resembling the behavior of LMNG. A comparable trend was observed among the unsymmetric GS-BTMs. BTM-C13,11, which forms relatively large aggregates, showed the greatest increases in aggregate in aggregate size with detergent concentration, while GS-BTM-C15,9, forming small aggregates, exhibited the least variation. Although additional examples and further studies are required to determine whether this trend is broadly applicable, the data suggest an interesting relationship between aggregate size and its sensitivity to concentration changes. This trend may reflect differences in self-assembly morphology. Specifically, detergents that form large, rod-like aggregates may respond to increased detergent concentration by elongating existing assemblies. In contrast, detergents forming small, globular micelles likely respond by forming more micelles rather than growing in size.[9] We also examined the impact of temperature on aggregate size by varying the solution temperature from 15 °C to 65 °C (**Fig. 3d**). Detergents that form small aggregates, such as DDM, GS-BTM-C10, and GS-BTM-C15,9, showed negligible variation in aggregate size across the temperature range. In contrast, detergents that form large aggregates, as exemplified by LMNG, BTM-C11, GS-BTM-C11, GS-

BTM-C12, and GS-BTM-C13,11, displayed more pronounced temperature-dependent changes in aggregate size. Interestingly, LMNG differed from the other large aggregate-forming detergents, by exhibiting a steady decrease in aggregate size with temperature. Taken together, these findings suggest that both concentration- and temperature-dependent variations in aggregate size can be, to some extent, predicted based on the inherent aggregate sizes of the detergent.

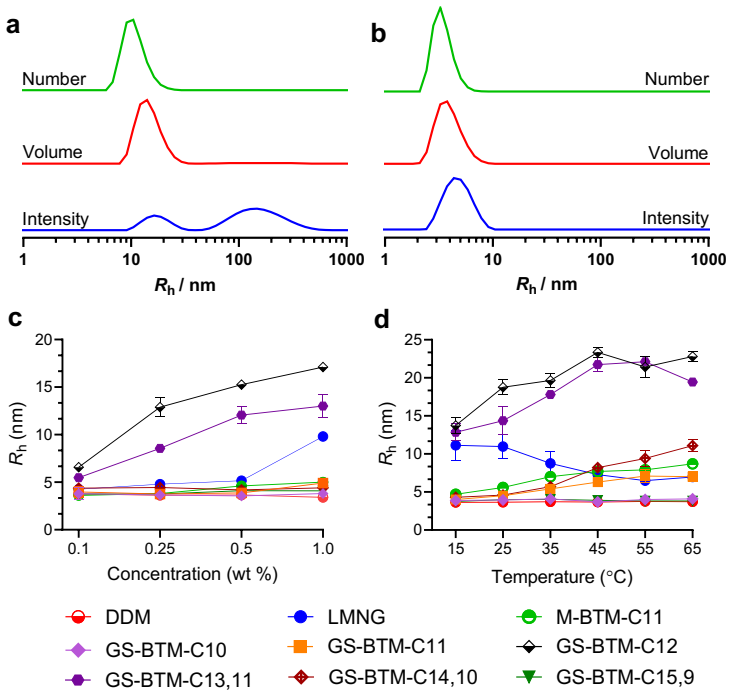


Figure 3. (a,b) Number-, volumne-, and intensity-weighted DLS profiles of (a) GS-BTM-C11 and (b) GS-BTM-C15,9. (c,d) Aggregate size variations of the GS-BTMs and control detergents (DDM, LMNG and BTM-C11) as a function of (c) detergent concentration and (d) solution temperature. In (c), aggregate sizes were measured at 25 °C across a detergent concentration range of 0.1–1.0 wt%. In (d), sizes were estimated at a fixed detergent concentration of 1.0 wt% while the solution temperature was increased from 15°C to 65 °C. Aggregate sizes are presented as hydrodynamic radii (R_h; z-average). Error bars represent the SEM; n = 4–5.

Detergent evaluation with membrane proteins To evaluate the potential of the group-swapped BTMs as tools for membrane protein research, we first tested their ability to stabilize the human β_2 adrenergic receptor (β_2AR), a prototypical GPCR.[42] β_2AR, initially purified in LMNG, was diluted into buffer

containing one of the test detergents,GS-BTMs, BTM-C11, LMNG, or DDM at a final detergent concentration of 0.1 wt%. This detergent exchange method results in mixed micelles surrounding the receptor, in which residual LMNG remain constant across all samples. Therefore, although residual LMNG could influence receptor stability, its uniform presence allows for a direct comparison of the effects of the tested detergents.[8] The receptor samples were incubated at room temperature for 7 days and the functional integrity of the receptor was assessed by monitoring the ability to bind the radioactive antagonist ([^{3}H]-dihydroalprenolol (DHA)) at regular intervals (**Figure 4**).[43-45] As expected, LMNG significantly outperformed DDM in maintaining receptor stability over time. Notably, BTM-C11 demonstrated superior performance even compared to LMNG, an important finding since GPCRs had not been included in our previous BTM evaluation. This result suggests that the BTM detergents could be valuable tools for GPCR structural studies. Among the symmetric GS-BTMs, receptor stabilization efficacy tended to increase with their alkyl chain length: GS-BTM-C11/C12 outperformed GS-BTM-C10 and were comparable or better than BTM-C11. Strikingly, the unsymmetric GS-BTMs provided even greater receptor stability, with GS-BTM-C14,10 and GS-BTM-15,9 exhibiting the highest performance. These results underscore the significant impact of both group-swapping and detergent unsymmetry on GPCR stability and highlight the potential of the GS-BTM scaffold for advancing membrane protein research.

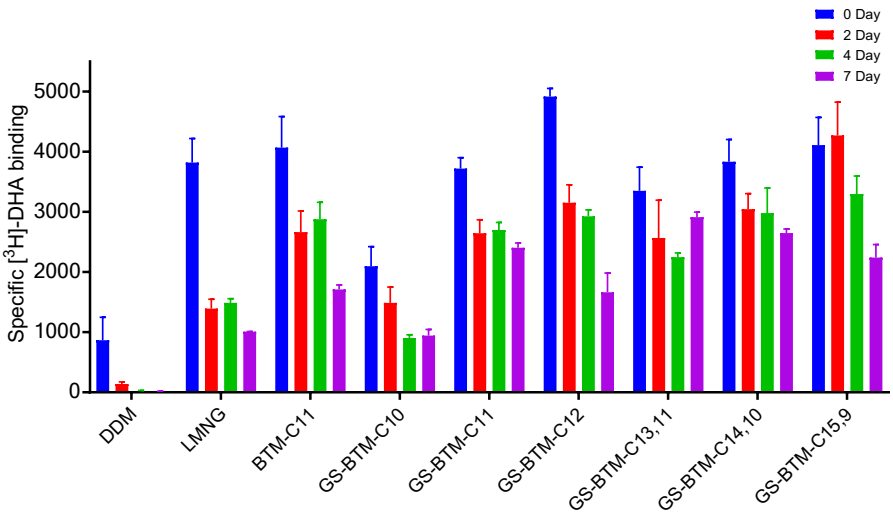


Figure 4. Long-term stability of β_2AR in the GS-BTMs. Control detergents (DDM, LMNG, and BTM-C11) were included for comparison, and all detergents tested at a concentration of 0.1 wt%. Receptor stability was assessed by monitoring the binding ability of β_2AR to the radio-labeled antagonist [[^{3}H]-dihydroalprenolol (DHA)] over a 7-day incubation period at room temperature. Error bars represent the SEM, $n = 2$.

Next, the GS-BTMs were evaluated using $MelB_{St}$, a melibiose transporter from *Salmonella typhimurium*.[46-48] Membranes overexpressing $MelB_{St}$ were solubilized with 1.5 wt% of each detergent, GS-BTMs, DDM, LMNG, or BTM-C11, for 90 minutes at 0 °C. Following extraction, the samples were subjected to thermal stress by incubation at elevated temperatures (45, 55, or 65 °C) for an additional 90 minutes. After thermal treatment, detergent-solubilized protein fractions were separated via ultra-centrifugation, and the levels of soluble $MelB_{St}$ quantified by Western blot analysis and densitometry. Because $MelB_{St}$ is prone to temperature-induced aggregation, the retention of soluble protein across the temperature gradient reflects both detergent efficiency in protein extraction and, more importantly, its ability to maintain protein stability under thermal stress.[19] At 0 °C, DDM extracted $MelB_{St}$ efficiently from the membranes, achieving nearly quantitative solubilization (**Figure 5**). LMNG and the original BTM-C11 also demonstrated high extraction efficiency. Notably, all GS-BTMs, regardless of symmetry, matched DDM in extraction performance, confirming that the GS-BTM architecture is well-suited for membrane protein solubilization. Upon incubation at 45 °C, all detergents including GS-BTMs, DDM, LMNG and BTM-C1, maintained the comparable levels of soluble MelB to those observed at 0 °C. However, a marked divergence in performance emerged at 55 °C. Under these more stringent conditions, DDM retained only ~10% $MelB_{St}$ in soluble form, indicating significant protein aggregation. BTM-C11 and LMNG showed better performance, retaining ~50% and ~70% soluble $MelB_{St}$, respectively. In contrast, all GS-BTMs, – both symmetric and unsymmetric, preserved nearly 100% of soluble $MelB_{St}$, with GS-BTM-C15,9 showing the highest protein stabilization efficacy. Interestingly, the unsymmetric GS-BTMs consistently outperformed the symmetric counterpart in thermal stability assays, reinforcing the utility of detergent unsymmetry as a design strategy. At 65 °C, most detergents failed to retain any soluble $MelB_{St}$, reflecting extensive protein aggregation. Remarkably, however, GS-BTM-C15,9 retained approximately 10% soluble protein even under this harsh condition. These results strongly support group-swapping and detergent unsymmetry as viable and effective approaches for enhancing detergent performance in membrane protein extraction, solubilization, and stabilization.

Commented [BB1]: `Looks to me as 100% or higher.

Commented [BB2]: Notably the GS-BTM-C15,9 gives almost 25% higher recovery than was in the unsolubilised membranes. Any comments as to why?

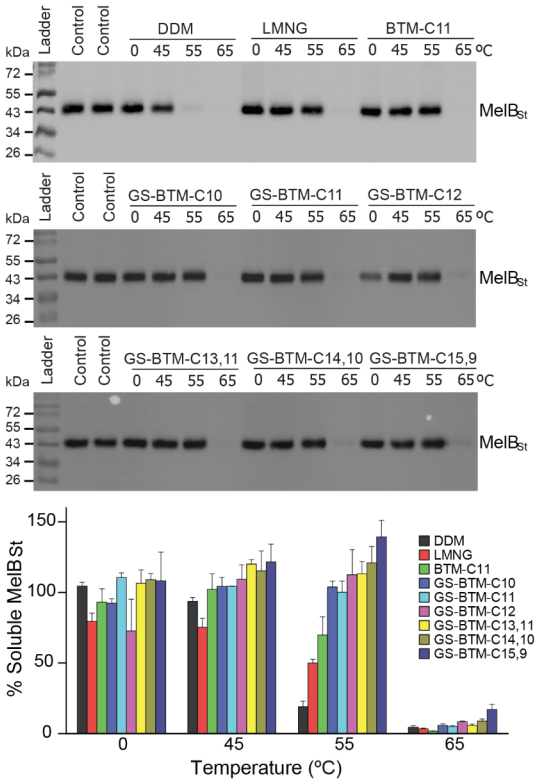


Figure 5. Thermo-stability of $MelB_{St}$ solubilized in the GS-BTMs and control detergents (DDM, LMNG, and BTM-C11). Top panel: Western blot analysis. Bottom panel: Quantification of soluble $MelB_{St}$ shown as a histogram. The amount of soluble $MelB_{St}$ in detergent extracts (0 °C) and thermally treated samples (45, 55, or 65 °C) were analyzed by SDS-PAGE followed by Western-blotting. The amounts of soluble $MelB_{St}$ obtained in each detergent were expressed as a percentage of the total $MelB_{St}$ in untreated membranes (defined as 'control'). Error bars represent the SEM, $n = 3$.

Discussion

Many novel detergents have been developed using entirely new molecular scaffolds, resulting in chemical structures that differ significantly from those of previously reported detergents. Given the structural diversity, it is expected that the new detergents also exhibit markedly different behaviors in stabilizing membrane proteins. In contrast to such scaffold-driven innovation, the current study adopts a different strategy – introducing a series of structurally related detergents by simply swapping the positions of the

detergent head and tail groups around the central linker (BT) in the previously developed BTMs. This modification retains the same number of head and tail groups as the original BTMs and thus, preserves the hydrophilic-lipophilic balance (HLB). By contrast, this group-swapping alters the connection points of the head and tail groups, shifting from the terminal primary to the internal secondary alcohols and the converse, potentially changing the critical packing parameter (CPP) of the detergent.[41] However, the CPP variation looks relatively small, based on the small R_h difference detected between BTM-C11 and GS-BTM-C11 (4.7 *vs* 4.9 nm). A small difference was also observed for water-solubility (~10 vs > 10 wt%) and CACs (8 *vs.* 9 μM). When we examined the impact of this minimal structural change (i.e. group-swapping) on membrane protein stabilization, GS-BTM-C11 outperformed the original counterpart (BTM-C11) in stabilizing both β_2AR and MelB. This finding demonstrates that group-swapping is a viable and effective strategy to enhance detergent efficacy for membrane protein stabilization. The comparative analysis between BTM-C11 and GS-BTM-C11 illustrates that even minor structural change can lead to measurable differences in detergent properties (e.g., CAC, micelle sizes), which can, in turn, result in substantial differences in detergent biological performance. This progression from small structural differences to observable property changes to substantial effects on biological function, underscores the importance of understanding detergent structure-property-efficacy relationships. Such behavior is attributable to the fact that detergents function as self-assembled aggregates in aqueous solution, rather than as individual molecules. Minor chemical changes leading to major changes in activity is also seen in enantiomeric stereoisomers, which are nearly identical in structure, but exhibit markedly different biological effects upon interacting with proteins, originating from their chirality. Therefore, understanding detergent efficacy for protein stabilization requires consideration of the collective interactions among detergent molecules and between detergent and membrane protein within protein-detergent complexes (PDCs).

In addition to head/tail group swapping, we further modified the GS-BTM scaffold by introducing detergent unsymmetry through incorporation of two different alkyl chains, while maintaining the total number of carbon atoms in the hydrophobic region. This approach preserves the HLB, resulting in the same value (12.3) for all unsymmetric GS-BTMs, as in the parent GS-BTM-C12. Despite retaining the same HLBs, the unsymmetric GS-BTMs exhibit lower CACs and notably smaller aggregate sizes. More importantly, the unsymmetric GS-BTMs showed improved performance in solubilizing and stabilizing membrane proteins compared to the symmetric counterparts. Thus, detergent unsymmetry emerges as an effective strategy for improving detergent behavior, as demonstrated in previous studies on unsymmetric MNGs. GS-BTM-C14,10 and GS-BTM-C15,9 showed optimal performance in supporting membrane protein solubility and stability. It is particularly noteworthy that detergent unsymmetry significantly reduced detergent aggregate sizes – a desirable feature for membrane protein structural study. Smaller self-assemblies are also beneficial in improving the water-solubility of detergents. Poor water solubility is a common issue in detergent development for membrane protein study. Unlike other strategies to increase water solubility, such as shortening alkyl chains or enlarging hydrophilic groups, which can alter HLB and negatively impact protein-detergent interactions, detergent unsymmetry offers a unique advantage. It enhances *detergent-detergent* interactions, contributing to the formation of stable micelles and,

consequently, better stabilization of membrane proteins. Increased *detergent-detergent* interactions is supported by the lower CMC observed for GS-BTM-C15,9 compared to its symmetrical counterpart (5 *vs.* 7 μM). Detergent unsymmetry could be particularly useful for improving the performance of symmetric detergents with short hydrophobic lengths. Such detergents often fail to stabilize membrane proteins due to inadequate hydrophobic matching with protein hydrophobic surfaces. A representative case is OGNG, a GNG with two hexyl chains (C6), which has been shown to be less effective than DDM in membrane protein stability. Introducing unsymmetry into such short-chained detergents could significantly enhance their performance in membrane protein stabilization, an idea currently under investigation. Given that OGNG has already been used in structural studies of 10 membrane proteins, the improved versions are likely to have broad applicability in further studies.[9] Overall, detergent unsymmetry represents a versatile and powerful strategy that can applied to a wide range of newly developed symmetric detergents not only to improve water-solubility, but also to enhance overall performance in membrane protein stabilization

Conclusion

In this study, we demonstrated that GS-BTM-C11 outperforms the original BTM-C11 in stabilizing membrane proteins, highlighting that even a minimal structural modification can have a significant impact on detergent efficacy for membrane protein stability. Furthermore, by applying the recently emerged concept of detergent unsymmetry to GS-BTM-C12, we developed three unsymmetric GS-BTMs, among which GS-BTM-C15,9 exhibited further superior performance in membrane protein stabilization. Notably, this detergent outperformed LMNG in both solubilization and stabilization of membrane proteins, suggesting its broad potential for applications in membrane protein manipulation, including extraction, purification, and structural studies. The structural strategies employed in this work, head/tail group-swapping and detergent unsymmetry, can be applied to other classes of detergents. Thus, this study not only introduces effective new detergent tools effective for membrane protein research but also presents versatile design strategies for enhancing the protein stabilization capability of detergent molecules.

ACKNOWLEDGMENT

This work was supported by the National Research Foundation of Korea (NRF) (2021R1A2C2006067 and 2018R1A6A1A03024231 to P.S.C.) and by the National Institutes of Health (NIH) (R35GM153222 to L.G.).

References

1. W. Cho and R. V. Stahelin, *Annu. Rev. Biophys. Biomol. Struct.*, 2005, **34**, 119-151.
2. K. Yadav, A. Yadav, P. Vashistha, V. P. Pandey and U. N. Dwivedi, *Curr. Protein Pept. Sci.*, 2019, **20**, 1226-1245.
3. Y. W. Lee, D. C. Luther, J. A. Kretzmann, A. Burden, T. Jeon, S. Zhai and V. M. Rotello, *Theranostics*, 2019, **9**, 3280-3292.
4. X. Qin, C. Yu, J. Wei, L. Li, C. Zhang, Q. Wu, J. Liu, S. Q. Yao and W. Huang, *Adv. Mater.*, 2019, **31**, e1902791.
5. H. Stahlberg, D. Fotiadis, S. Scheuring, H. Remigy, T. Braun, K. Mitsuoka, Y. Fujiyoshi and A. Engel, *FEBS Lett.*, 2001, **504**, 166-172.

6. H. Yin and A. D. Flynn, *Annu. Rev. Biomed. Eng.*, 2016, **18**, 51-76.
7. K. R. Vinothkumar and R. Henderson, *Q. Rev. Biophys.*, 2010, **43**, 65-158.
8. V. Kotov, K. Bartels, K. Veith, I. Josts, U. K. T. Subhramanyam, C. Gunther, J. Labahn, T. C. Marlovits, I. Moraes, H. Tidow, C. Low and M. M. Garcia-Alai, *Sci. Rep.*, 2019, **9**, 10379.
9. H. J. Lee, H. S. Lee, T. Youn, B. Byrne and P. S. Chae, *Chem*, 2022, **8**, 980-1013.
10. (a) R. M. Garavito and S. Ferguson-Miller, *J. Biol. Chem.*, 2001, **276**, 32403-32406; (b) F. Magnani, Y. Shibata, M. J. Serrano-Vega and C. G. Tate, *PNAS*, 2008, **105**, 10744-10749; (c) S. Newstead, S. Ferrandon and S. Iwata, *Protein Sci.*, 2008, **17**, 466-472; (d) J. L. Parker and S. Newstead, *Protein Sci.*, 2012, **21**, 1358-1365; (e) Y. He, K. Wang and N. Yan, *Protein Cell*, 2014, **5**, 658-672.
11. S. Faham and J. U. Bowie, *J. Mol. Biol.*, 2002, **316**, 1-6.
12. C. Tribet, R. Audebert and J. L. Popot, *PNAS*, 1996, **93**, 15047-15050.
13. C. L. McGregor, L. Chen, N. C. Pomroy, P. Hwang, S. Go, A. Chakrabartty and G. G. Prive, *Nat. Biotechnol.*, 2003, **21**, 171-176.
14. H. Tao, S. C. Lee, A. Moeller, R. S. Roy, F. Y. Siu, J. Zimmermann, R. C. Stevens, C. S. Potter, B. Carragher and Q. Zhang, *Nat. Methods*, 2013, **10**, 759-761.
15. J. Frauenfeld, R. Loving, J. P. Armache, A. F. Sonnen, F. Guettou, P. Moberg, L. Zhu, C. Jegerschold, A. Flayhan, J. A. Briggs, H. Garoff, C. Low, Y. Cheng and P. Nordlund, *Nat. Methods*, 2016, **13**, 345-351.
16. A. Nath, W. M. Atkins and S. G. Sligar, *Biochemistry*, 2007, **46**, 2059-2069.
17. J. M. Dorr, S. Scheidelaar, M. C. Koorengevel, J. J. Dominguez, M. Schafer, C. A. van Walree and J. A. Killian, *Eur. Biophys. J.*, 2016, **45**, 3-21.
18. A. A. Gulamhussein, R. Uddin, B. J. Tighe, D. R. Poyner and A. J. Rothnie, *Biochim. Biophys. Acta, Biomembr.*, 2020, **1862**, 183281.
19. P. S. Chae, S. G. Rasmussen, R. R. Rana, K. Gotfryd, R. Chandra, M. A. Goren, A. C. Kruse, S. Nurva, C. J. Loland, Y. Pierre, D. Drew, J. L. Popot, D. Picot, B. G. Fox, L. Guan, U. Gether, B. Byrne, B. Kobilka and S. H. Gellman, *Nat. Methods*, 2010, **7**, 1003-1008.
20. P. S. Chae, R. R. Rana, K. Gotfryd, S. G. Rasmussen, A. C. Kruse, K. H. Cho, S. Capaldi, E. Carlsson, B. Kobilka, C. J. Loland, U. Gether, S. Banerjee, B. Byrne, J. K. Lee and S. H. Gellman, *Chem. Commun.*, 2013, **49**, 2287-2289.
21. P. S. Chae, S. G. Rasmussen, R. R. Rana, K. Gotfryd, A. C. Kruse, A. Manglik, K. H. Cho, S. Nurva, U. Gether, L. Guan, C. J. Loland, B. Byrne, B. K. Kobilka and S. H. Gellman, *Chem. Eur. J.*, 2012, **18**, 9485-9490.
22. Q. Zhang, X. Ma, A. Ward, W. X. Hong, V. P. Jaakola, R. C. Stevens, M. G. Finn and G. Chang, *Angew. Chem. Int. Ed. Engl.*, 2007, **46**, 7023-7025.
23. S. C. Howell, R. Mittal, L. Huang, B. Travis, R. M. Breyer and C. R. Sanders, *Biochemistry*, 2010, **49**, 9572-9583.
24. S. C. Lee, B. C. Bennett, W. X. Hong, Y. Fu, K. A. Baker, J. Marcoux, C. V. Robinson, A. B. Ward, J. R. Halpert, R. C. Stevens, C. D. Stout, M. J. Yeager and Q. Zhang, *PNAS*, 2013, **110**, E1203-1211.
25. K. A. Nguyen, M. Peuchmaur, S. Magnard, R. Haudecoeur, C. Boyere, S. Mounien, I. Benammar, V. Zampieri, S. Igonet, V. Chaptal, A. Jawhari, A. Boumendjel and P. Falson, *Angew. Chem. Int. Ed. Engl.*, 2018, **57**, 2948-2952.
26. J. Dauvergne, E. M. Desuzinges, C. Faugier, S. Igonet, M. Soulié, E. Grousson, D. Cornut, F. Bonneté, G. Durand, E. Dejean and A. Jawhari, *Chemistryselect*, 2019, **4**, 5535-5539.
27. L. H. Urner, A. Ariamajd and A. Weikum, *Chem. Sci.*, 2022, **13**, 10299-10307.
28. F. Zhao, Z. Zhu, L. Xie, F. Luo, H. Wang, Y. Qiu, W. Luo, F. Zhou, D. Xue, Z. Zhang, T. Hua, D. Wu, Z. J. Liu, Z. Le and H. Tao, *Chemistry*, 2022, **28**, e202201388.
29. M. Yang, W. Luo, W. Zhang, H. Wang, D. Xue, Y. Wu, S. Zhao, F. Zhao, X. Zheng and H. Tao, *Chem. Asian J.*, 2022, **17**, e202200372.
30. L. H. Urner, F. Junge, F. Fiorentino, T. J. El-Baba, D. Shutin, G. Nolte, R. Haag and C. V. Robinson, *Chemistry*, 2023, **29**, e202300159.
31. S. Yoon, H. E. Bae, P. Hariharan, A. Nygaard, B. Lan, M. Woubshete, A. Sadaf, X. Liu, C. J. Loland, B. Byrne, L. Guan and P. S. Chae, *Bioconjugate Chem.*, 2024, **35**, 223-231.
32. M. Das, Y. Du, J. S. Mortensen, O. Ribeiro, P. Hariharan, L. Guan, C. J. Loland, B. K. Kobilka, B. Byrne and P. S. Chae, *Chem. Sci.*, 2017, **8**, 1169-1177.
33. M. Das, F. Mahler, P. Hariharan, H. Wang, Y. Du, J. S. Mortensen, E. P. Patallo, L. Ghani, D. Glück and H. J. Lee, *J. Am. Chem. Soc.*, 2020, **142**, 21382-21392.

34. H. Cui, A. G. Cheetham, E. T. Pashuck and S. I. Stupp, *J. Am. Chem. Soc.*, 2014, **136**, 12461-12468.
35. E. K. Perttu, A. G. Kohli and F. C. Szoka Jr, *J. Am. Chem. Soc.*, 2012, **134**, 4485-4488.
36. R. Gimeno-Ferrero, V. Valdivia, I. Fernández, M. L. García-Martín and M. Pernia Leal, *Sci. Rep.*, 2024, **14**, 28887.
37. H. E. Bae, Y. Du, P. Hariharan, J. S. Mortensen, K. K. Kumar, B. Ha, M. Das, H. S. Lee, C. J. Loland, L. Guan, B. K. Kobilka and P. S. Chae, *Chem. Sci.*, 2019, **10**, 1107-1116.
38. M. Ehsan, L. Ghani, B. Lan, S. Katsube, I. H. Poulsen, X. Zhang, M. Arslan, B. Byrne, C. J. Loland, L. Guan, X. Liu and P. S. Chae, *Chembiochem*, 2025, **26**, e202400958.
39. W. C. Griffin, *J. Soc. Cosmet. Chem.*, 1954, **5**, 249-256.
40. A. Chattopadhyay and E. London, *Anal. Biochem.*, 1984, **139**, 408-412.
41. J. Israelachvili, *Colloids Surf. A: Physicochem. Eng. Asp.*, 1994, **91**, 1-8.
42. D. M. Rosenbaum, V. Cherezov, M. A. Hanson, S. G. Rasmussen, F. S. Thian, T. S. Kobilka, H. J. Choi, X. J. Yao, W. I. Weis, R. C. Stevens and B. K. Kobilka, *Science*, 2007, **318**, 1266-1273.
43. S. E. Mansoor, H. S. McHaourab and D. L. Farrens, *Biochemistry*, 2002, **41**, 2475-2484.
44. G. Swaminath, J. Steenhuis, B. Kobilka and T. W. Lee, *Mol. Pharmacol.*, 2002, **61**, 65-72.
45. X. Yao, C. Parnot, X. Deupi, V. R. Ratnala, G. Swaminath, D. Farrens and B. Kobilka, *Nat. Chem. Biol.*, 2006, **2**, 417-422.
46. L. Guan, S. Nurva and S. P. Ankeshwarapu, *J. Biol. Chem.*, 2011, **286**, 6367-6374.
47. L. Guan and P. Hariharan, *Commun. Biol.*, 2021, **4**, 931.
48. P. Hariharan, Y. Shi, S. Katsube, K. Willibal, N. D. Burrows, P. Mitchell, A. Bakhtiiari, S. Stanfield, E. Pardon, H. R. Kaback, R. Liang, J. Steyaert, R. Viner and L. Guan, *Elife*, 2024, **12**, RP92462.